

Assessment of Wall Deflection Induced by Braced Excavation in Spatially Variable Soils via Convolutional Neural Network

Chongzhi Wu¹ and Wengang Zhang²

¹School of Civil Engineering, Chongqing University, Chongqing 400045, P. R. China.
E-mail: iwuchongzhi@cqu.edu.cn

²School of Civil Engineering, Chongqing University, Chongqing 400045, P. R. China.
E-mail: zhangwg@cqu.edu.cn

Abstract: Recently, the random field finite element method (RF-FEM) has attracted significantly increasing attention in the field of geotechnical engineering, especially for the purpose of analyzing the response of geotechnical systems due to the inherent variability of physical and mechanical properties. However, the method requires repeated finite element calculations based on a mass of sampling processes, making the computing effort expensive. The surrogate model is one of the techniques commonly adopted to alleviate the computational burden. In addition, some architectures of deep learning surrogate models are so unique that it is difficult to transfer to similar cases and to be familiar and reproducible by readers. In this study, we propose a convolutional neural network (CNN) surrogate model based on classical architecture, VGG6, to perform random field finite element analyses (RF-FEM). We pre-process the tabular data generated by the random field method into an image-like format as input data. The VGG6 is used as a surrogate model to replace the original RF-FEM simulations for all subsequent calculations. The applications of the proposed method to assess wall deflection of braced excavation in clays with randomly varying cohesion c_u and the friction angle φ are illustrated and compared in different cases. The excellent agreement between the VGG6 outputs and the FEM predictions demonstrated the promising potential of using VGG6s as a surrogate model for reliability analysis in spatially variable soils. Moreover, the model saves a lot of computing time and computing power and fully proves the generalization performance of the model under various cases.

Keywords: Random field finite element method; Surrogate model; Convolutional neural network; VGG6; Wall deflection of braced excavation.

1 Introduction

In the past few decades, many researchers have contributed to reliability analysis of geo-structures. The random field finite element method (RF-FEM) proposed by (Griffiths and Fenton, 2004) has been widely used in geotechnical reliability analysis, in which the spatially variable soil can be rationally and explicitly characterized. To deal with low failure probability level, Gong et al. proposed a new efficient sample method for reliability analysis of deep excavation (Gong et al., 2017). Goh et al. focused on reliability analysis for basal heave of deep excavation in spatial variable soil layers (Goh et al., 2019). Luo et al. adopted Cholesky decomposition method and PLAXIS 2D software to generate 2-D random finite element models of deep excavation (Luo et al., 2018). Furthermore, some studies pointed that spatial variability of soil parameters had a negative influence on deformations and struts forces of deep excavations (Qin et al., 2021). Gholampour et al. presented a practical approach for reliability analysis of braced excavation in spatially varied unsaturated soils (Gholampour and Johari, 2019). However, the RF-FEM generally requires a large number of simulations for guaranteeing the estimate with the desired accuracy. Although most of the commercial geotechnical software such as ABAQUS and PLAXIS provides a powerful tool for conducting finite element analysis, it may be a prohibitively expensive task to perform a huge number of deterministic finite element analyses in geotechnical engineering applications.

As an alternative, many approaches have been proposed to facilitate the RF-FEM of the excavation, such as first-order reliability method (FORM) (Cho, 2007), subset simulation (SS) (Cao et al., 2017; Wang et al., 2010), response surface method (RSM) and their advanced variants (Li et al., 2016). However, many scholars also found that these methods may lead to unsatisfactory results the prior assumption on the structures of performance functions (Wang et al., 2020), or may suffer from the curse of dimensionality in high degree of inherent spatial variability problems and so on. With rapid development of artificial intelligence technologies, many researchers have attempted to integrate machine learning (ML) algorithms with geotechnical reliability analysis for alleviating computational burden (Jong et al., 2021).

Recently, various ML algorithms and their variants have been successfully applied in the geotechnical reliability analysis, such as multivariate adaptive regression splines (MARS) e.g., (Liu and Cheng, 2016; Zhang et al., 2021a), extreme gradient boosting (XGBoost) e.g., (Wang et al., 2020), and convolutional neural network (CNN) (Wang Ze Zhou, 2022). The main idea of CNN in implementing reliability analysis is to reconstruct the high-dimensional implicit performance function through learning from the prepared data which mainly consists

of the input images that contain the information about the spatially variable soil parameters in the form of pixels and the corresponding response of interest. As the established CNN model after sufficient training and proper validation, it can be conveniently used to perform the computationally demanding RF-FEM analyses. However, the parameters of the CNN architecture used in these studies are generally unconventional, and many studies have used trial-and-error method and guided by checking against the results presented in the CNN's architecture parameters (Wang and Goh, 2021), so that a lot of computational experimentations are needed to derive these unconventional architecture parameters. This seems to defeat the purpose of building a surrogate model for us to save time and computing power. In addition, this is also not conducive to being applied to similar cases and not easy for other scholars to use for reference and engineering application. Therefore, we modified the classical CNN architecture, VGG16 (Simonyan and Zisserman, 2014), and fixes the value of the hyperparameters, and then combines different cases to check the accuracy and robustness of the model, so that the model can provide reference and guidance for engineers and other researchers.

2 Random field modeling of spatially variable soil properties

In this study, the diaphragm wall deflections in the braced excavation are analyzed by the geotechnical finite element method using PLAXIS 2D. Figure 1 shows the two dimensions of the finite element model (FEM). Because of the symmetry of the model, only the left half of the excavation is modeled. This example refers to the case presented by (Goh et al., 2019). In the FEM simulation, since a large number of sampling calculations is required, for computational efficiency, the soil bodies are simulated via 6-noded elements. In addition, considering that this paper mainly studies the efficient surrogate model of the stochastic finite element model, the Mohr-Coulomb model (MC) and hardening soil model with harden stiffness (HS) are used to simulate clay soil and sandy soil, respectively, which can make the problem is appropriately simplified. For clay soil, the cohesion, friction angle and elastic modulus is 30 kPa, 20° , 9MPa, respectively. For sand soil, the cohesion, friction angle and dilation angle are 0 kPa, 32° , 2° , respectively.

In this paper, we consider two levels of coefficient of variation (COV) of cohesion ($COV_{c_u} = 20\%$, 30%), three levels of friction angle ($COV_{\phi} = 10\%$, 15% , 20%) (Phoon and Ching, 2015), which orthogonal combine these working condition, so the six RF-FEM conditions groups' data can be obtained. Table 1 summarizes the parameters involved in this study. The scale of fluctuation (SOF) is the critical parameter to describe the soil spatial variability (Zhang et al., 2022). Here, according to the size of the FEM model, we take the vertical scale of fluctuation $\delta y = 2.5\text{m}$ and the horizontal scale of fluctuation $\delta x = 25\text{m}$ (Jiang et al., 2015). For each Group, RF-FEM analyses were carried out with 500 Latin hypercube samples, because it can be known from **Figure 2** that the mean and standard deviation of the wall deflection tend to be stable with the increase of the number of simulations, and it has stabilized at 500. The results of the maximum deflection of the diaphragm wall from the 500 Latin hypercube samples are subsequently adopted as the training and testing dataset.

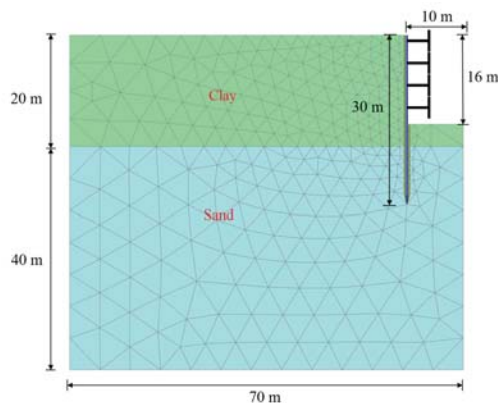


Figure 1. Finite-element model for deflections analysis of a diaphragm wall.

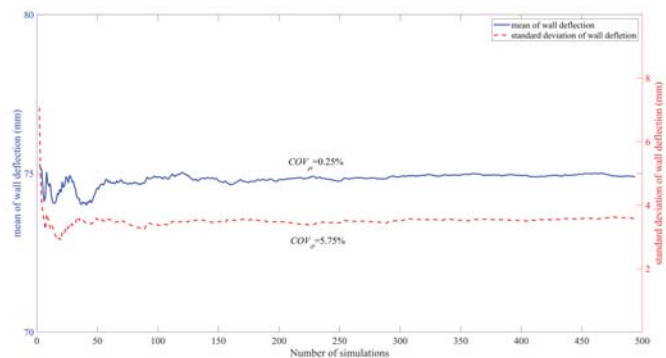


Figure 2. Convergence curve of the wall deflection (Group 1)

Table 1. Arrangement of parameters in cases.

Group	Parameter	Mean	COV	Distribution	SOF	
					δ_y (m)	δ_x (m)
Group 1	c_u (kPa)	30	30%	Lognormal	2.5	25
	φ (°)	20	10%			
Group 2	c_u (kPa)	30	30%	Lognormal	2.5	25
	φ (°)	20	15%			
Group 3	c_u (kPa)	30	30%	Lognormal	2.5	25
	φ (°)	20	20%			
Group 4	c_u (kPa)	30	20%	Lognormal	2.5	25
	φ (°)	20	10%			
Group 5	c_u (kPa)	30	20%	Lognormal	2.5	25
	φ (°)	20	15%			
Group 6	c_u (kPa)	30	20%	Lognormal	2.5	25
	φ (°)	20	20%			

COV: Coefficient of variation

SOF: Scale of fluctuation, δ_y - vatical scale of fluctuation; δ_x - horizontal scale of fluctuation

3 Architecture of proposed CNN

3.1 Input layer

The data generated by the RF-FEM is tabular data with a size of 500 rows (500 Latin hypercube sampling) \times 560 columns (560 RF-FEM elements). However, CNN generally deals with image data, so we need to process the data into an image-like format. As shown in Figure 3. Firstly, 560 columns of 1 row can be reshaped into a matrix of 20 rows and 28 columns, in other words, each random field is described by a matrix of the size of 20×28 , and 500 such matrices can be obtained by repeating 500 times. Then the two matrices (cohesion c_u and friction angle φ) are superposed together in the spatial direction to form a three-dimensional tensor, which is expressed as $[[[2, 20, 28]]]$ by the tensor, where 20×28 is the size of the image and 2 is the color channel of the images. Finally, all the data can be expressed as a four-dimensional tensor, namely $[[[[500, 2, 20, 28]]]]$. As for the input layer, which is selected from the four-dimensional tensor according to different cases.

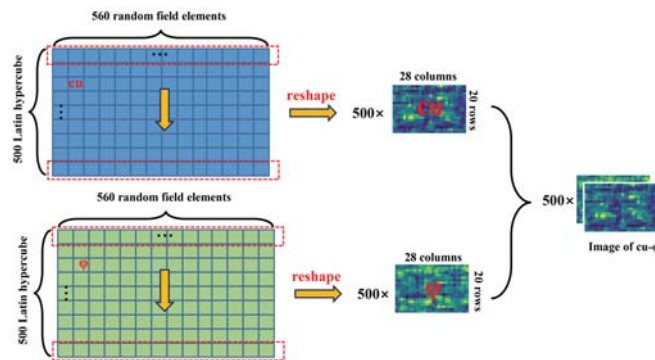


Figure 3. The process of the tabular data reshapes to the image-like format

3.2 Architecture of established CNN model

Figure 4 shows the architecture of the proposed CNN model. It is important to emphasize that this architecture does not require constant trial-and-error to determine the final CNN model, but rather uses the same architecture and hyperparameters. This architecture is adapted from the famous VGG16 architecture (Simonyan and Zisserman, 2014). VGG16 gets its name from having 13 convolutional layers and 3 fully connected layers, which can be expressed by a formula: [input \rightarrow (convolutional \times 2+pooling) \times 2 \rightarrow (convolutional \times 3+pooling) \times 3 \rightarrow fully connected \times 3 \rightarrow output]. The input layer of VGG16 is of fixed size 224×224 RGB image, but the input layer is fixed size 20×28 image, which cannot go through so many layers, so our architecture is transformed to [input \rightarrow (convolutional \times 2+pooling) \times 2 \rightarrow fully connected \times 2 \rightarrow output], which has six layers, so we call it VGG6 for convenience. The input layer is an image of size $20 \times 28 \times 2$, and the outputs produced by the convolutional layer, which consisted of 64 filters of size 3, padding of 1, and a stride of 1, were fed into the ReLU layer, repeat twice. It can be noticed that during this process, the size of the image is kept at 20×28 . A pooling layer with a size of 2 and a stride of 2 makes the size of the image reduce by half to 10×14 , and then the image is further processed by the same parameters two convolutional layers and one pooling layer. Finally, the regression layer is constructed between the wall deflections and the outputs of the two fully-connected layers.

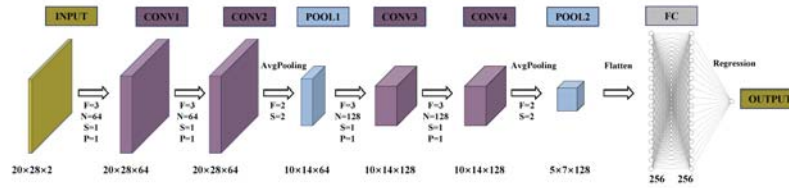


Figure 4. The architecture of the VGG6 (F: Filter size; N: Number of filters; P: Padding; S: Stride).

4 Cases and results

4.1 The first case

As mentioned above, there are 6 Groups of RF-FEM conditions, and each Group has 500 samples, as shown in Table 1. Combine different cases according to the 6 Groups' random field samples. In the first case, Since the 500 samples themselves is random, there is no need to deliberately choose the training set and testing set. The first 200 samples of each Group are taken as the training set, the last 300 samples are taken as the testing set, and the predicted label is the wall deflection.

To quantitatively evaluate and compare these models' performance, the coefficient of determinations (R^2) and the root mean squared error (RMSE) of the 6 models in the testing set were compared in Figure 5. The x-coordinate is three levels of friction angle ($COV_\phi = 10\%, 15\%, 20\%$), and the y-coordinate is the coefficient of determinations (R^2) and RMSE, respectively, and two levels of COV of cohesion ($COV_{cu} = 20\%, 30\%$) is the red line and the blue line, respectively. It can see that the blue line is above the red line in Figure 5, suggesting that the R^2 of $COV_{cu} = 30\%$ is better than $COV_{cu} = 20\%$ because a larger R^2 means better fitting performance. However, this phenomenon seems to be the opposite of Figure 5 (right), and the RMSE of $COV_{cu} = 30\%$ larger than $COV_{cu} = 20\%$ (the larger RMSE value and the worse performance). We believe that the larger COV_{cu} and COV_ϕ lead to a greater standard deviation (their mean value is fixed) for the corresponding wall deflections, i.e. a flatter distribution, and that the RMSE is related to the numerical scale of the wall deflection itself. Therefore, the RMSE value tends to increase monotonically with the increase of the COV_{cu} and the COV_ϕ under a similar model.

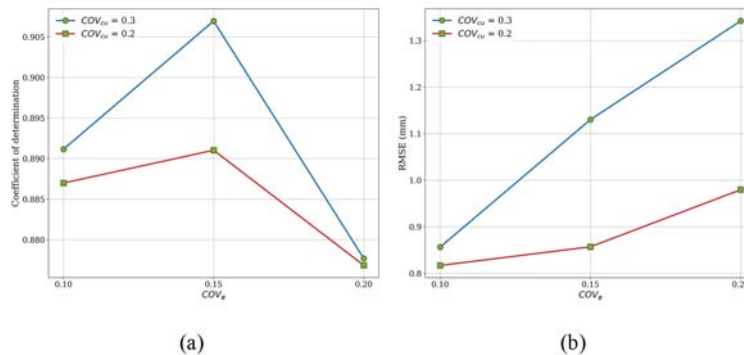


Figure 5. Effect of variations in three levels of friction angle on the two levels of COV of cohesion of different performance indicators: (a) the coefficient of determinations (R^2); (b) the root mean squared error (RMSE).

4.2 The second case

To further test the generalization ability of the model, a partial sample mixed case test was carried out on the condition that the architecture and hyperparameters of the original model were kept unchanged. In the second case, the first 50 samples, 100 samples, 150 samples, and 200 samples of each Group were respectively taken to form the training set, and the remaining samples of each Group formed the test set. In other words, the number of training sets will be 300 samples, 600 samples, 900 samples, and 1200 samples, and the corresponding test sets will be 2700 samples, 2400 samples, 2100 samples, and 1800 samples. As shown in Figure 6, RMSE decreased as the initial sample size increased, and larger R^2 values were obtained for larger initial sample sizes. This is a reasonable trend because more initial samples are involved in the training, CNNs can learn additional features pertaining to the intensity and spatial variation of the random parameter, therefore yielding improved predictions.

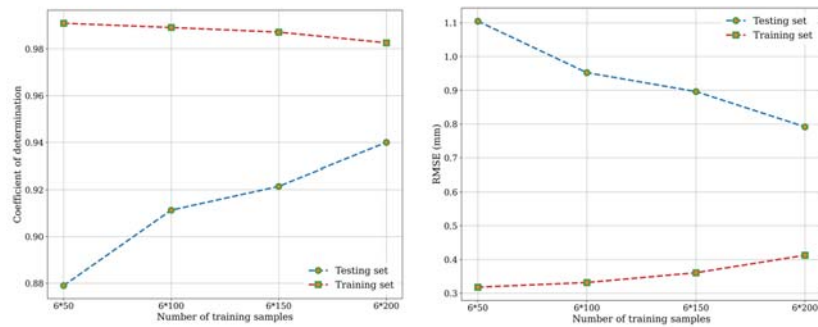


Figure 6. Effect of variations in the number of training samples on the training and testing set of different performance indicators: (a) the coefficient of determinations (R2); (b) the root mean squared error (RMSE).

4.3 The third case

Although this kind of surrogate model can greatly save time cost, it still needs to calculate part of the initial samples through FEM as the training set, which means that the calculation time of this part is unavoidable, which brings some troubles to our actual use. Therefore, we consider using all samples of one case as a training set to predict samples of other remaining cases and check out their predictive performance.

In the third case, we will introduce the XGBoost algorithm and let it combine with the Bayesian optimization algorithm for hyperparameter tuning to establish a surrogate model and compare it with the previously established CNN models. The Bayesian optimization algorithm plays the role of automatically selecting the hyperparameters of XGBoost, that is, the range of the input hyperparameters, so that the Bayesian optimization algorithm uses certain rules to find the optimal combination of hyperparameters, so that the model performs best. The specific principle can refer to this reference (Zhang et al., 2021b). Figure 7 (left) and Figure 7 (right) show the coefficient of determination and RMSE curves of CNN models and XGBoost models under different Groups used as training samples. It can be seen that the prediction accuracy of the XGBoost model is higher than that of the CNN model when Group 2 and Group 3 are used as training samples, but its prediction accuracy of other Groups is lower than that of the CNN model (The mean of the overall prediction accuracy is also lower than the CNN model), and its prediction accuracy fluctuates much more than CNN model in different Groups. It indicates that the overall CNN model is slightly better than the XGBoost model. However, we noticed that XGBoost also has its advantages, so we consider doing a simple average fusion of the two models, that is, multiplying the prediction results of the two models by 0.5 and adding up to get the new result as the final prediction result and calculate its final accuracy. As shown in Figure 7 (purple dotted line). It finds that the predicted results were significantly better than the results predicted by the respective models, and this advantage was reflected in each Group as a training set, suggesting that the mixed average model can well inherit the two models' respective the advantage is a very good hybrid model.

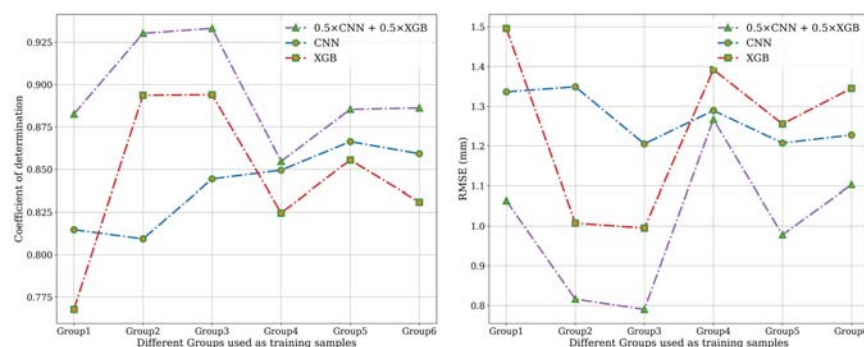


Figure 7. Effect of variations in the number of different Groups used as training samples on the CNN, XGBoost, and Averaging model of different performance indicators: (a) the coefficient of determinations (R2); (b) the root mean squared error (RMSE).

5 Conclusions

This study presented the application of the CNN model to efficiently predict the wall deflection of braced excavation considering the spatial variability of soil parameters. The validity of the proposed method was demonstrated through RF-FEM analyses performed for three cases. In addition, this study also introduced the XGBoost model and the proposed CNN model for comparative analysis and investigated the predictive performance of the fusion of the two models. The following conclusions can be drawn from this study:

(i) In general, the predicted wall deflection obtained from the established VGG6 models agrees well with those calculated from the RF-FEM results for three cases, indicating that the VGG6 models can provide satisfactory performance in the prediction of various combinations of cases, which offers a promising tool facilitate the wall deflection of braced excavation prediction in spatially variable soil parameters.

(ii) In the first case, the VGG6 models perform the worst when $COV_{\varphi}=20$. These two-evaluation metrics seem to contradict each other, so we need to look at these evaluation metrics dialectically. In the second case, with the increase of training samples, the accuracy of the VGG6 models on the test set also increases accordingly, while the accuracy on the training set has a downward trend, indicating that more training samples can improve generalization performance and reduce overfitting. In the third case, a Group of RF-FEM sample data with COV values at the median should be selected as training samples as much as possible so that the model established in this way has higher relative accuracy and is unbiased.

(iii) The proposed VGG6 based on the classic CNN architecture can be trained to recognize high-level features that contain information about the random variabilities in both spatial distribution and intensity, from which they gain the capability to make good quality RF-FEM predictions. Due to the fixed basic architecture and hyperparameters, the model saves a lot of computing time and computing power and fully proves the generalization performance of the model under various cases.

(iv) Many machine learning algorithms based on tree models can also easily break the so-called curse of high dimensionality and are used in the RF-FEM surrogate model. However, its accuracy and stability are slightly inferior to the CNN-based model. After the average fusion of the two models, the performance of the new model obtained is better than the original two models, indicating that the two models have a certain complementarity.

Acknowledgments

We acknowledge the financial support from the National Natural Science Foundation of China (No. 52078086), Natural Science Foundation of Chongqing, China (cstc2020jcyj-jq0087) and High-end Foreign Expert Introduction program (No. G20200022005 and DL2021165001L).

References

- Cao, Z., Wang, Y., Li, D., 2017. Efficient Monte Carlo Simulation of Parameter Sensitivity in Probabilistic Slope Stability Analysis, in: Cao, Z., Wang, Y., Li, D. (Eds.), Probabilistic Approaches for Geotechnical Site Characterization and Slope Stability Analysis. Springer Berlin Heidelberg, Berlin, Heidelberg, pp. 169–184. https://doi.org/10.1007/978-3-662-52914-0_8
- Cho, S.E., 2007. Effects of spatial variability of soil properties on slope stability. *Eng. Geol.* 92, 97–109. <https://doi.org/10.1016/j.enggeo.2007.03.006>
- Gholampour, A., Johari, A., 2019. Reliability-based analysis of braced excavation in unsaturated soils considering conditional spatial variability. *Comput. Geotech.* 115, 103163. <https://doi.org/10.1016/j.compgeo.2019.103163>
- Goh, A.T.C., Zhang, W.G., Wong, K.S., 2019. Deterministic and reliability analysis of basal heave stability for excavation in spatially variable soils. *Computers and Geotechnics*. <https://doi.org/10.1016/j.compgeo.2018.12.015>
- Gong, W., Juang, C.H., Martin, J.R., 2017. A new framework for probabilistic analysis of the performance of a supported excavation in clay considering spatial variability. *Géotechnique* 67, 546–552. <https://doi.org/10.1680/jgeot.15.P.268>
- Griffiths, D.V., Fenton, G.A., 2004. Probabilistic slope stability analysis by finite elements. *J. Geotech. Geoenviron. Eng.*
- Jiang, S.-H., Li, D.-Q., Cao, Z.-J., Zhou, C.-B., Phoon, K.-K., 2015. Efficient System Reliability Analysis of Slope Stability in Spatially Variable Soils Using Monte Carlo Simulation. *Journal of Geotechnical and Geoenvironmental Engineering*. [https://doi.org/10.1061/\(asce\)gt.1943-5606.0001227](https://doi.org/10.1061/(asce)gt.1943-5606.0001227)
- Jong, S.C., Ong, D.E.L., Oh, E., 2021. State-of-the-art review of geotechnical-driven artificial intelligence techniques in underground soil-structure interaction. *Tunnelling and Underground Space Technology* 113, 103946. <https://doi.org/10.1016/j.tust.2021.103946>
- Li, D.Q., Xiao, T., Cao, Z.J., Zhou, C.B., Zhang, L.M., 2016. Enhancement of random finite element method in reliability analysis and risk assessment of soil slopes using Subset Simulation. *Landslides*.
- Liu, L.-L., Cheng, Y.-M., 2016. Efficient system reliability analysis of soil slopes using multivariate adaptive regression splines-based Monte Carlo simulation. *Comput. Geotech.* 79, 41–54. <https://doi.org/10.1016/j.compgeo.2016.05.001>
- Luo, Z., Hu, B., Wang, Y., Di, H., 2018. Effect of spatial variability of soft clays on geotechnical design of braced excavations: A case study of Formosa excavation. *Comput. Geotech.* 103, 242–253. <https://doi.org/10.1016/j.compgeo.2018.07.020>
- Phoon, K.K., Ching, J., 2015. Risk and reliability in geotechnical engineering.
- Qin, Y., Zhu, F., Xu, D., 2021. Effect of the spatial variability of soil parameters on the deformation behavior of excavated slopes. *Comput. Geotech.* 136, 104246. <https://doi.org/10.1016/j.compgeo.2021.104246>
- Simonyan, K., Zisserman, A., 2014. Very Deep Convolutional Networks for Large-Scale Image Recognition. *arXiv [cs.CV]*.
- Wang, L., Wu, C., Tang, L., Zhang, W., Lacasse, S., Liu, H., 2020. Efficient reliability analysis of earth dam slope stability using extreme gradient boosting method. *Acta Geotech.*
- Wang, Y., Cao, Z., Au, S.-K., 2010. Efficient Monte Carlo Simulation of parameter sensitivity in probabilistic slope stability analysis. *Comput. Geotech.* 37, 1015–1022. <https://doi.org/10.1016/j.compgeo.2010.08.010>

- Wang Ze Zhou, 2022. Deep Learning for Geotechnical Reliability Analysis with Multiple Uncertainties. *J. Geotech. Geoenviron. Eng.* 148, 06022001. [https://doi.org/10.1061/\(ASCE\)GT.1943-5606.0002771](https://doi.org/10.1061/(ASCE)GT.1943-5606.0002771)
- Wang, Z.Z., Goh, S.H., 2021. A maximum entropy method using fractional moments and deep learning for geotechnical reliability analysis. *Acta Geotech.* <https://doi.org/10.1007/s11440-021-01326-2>
- Zhang, J.Z., Zhang, D.M., Huang, H.W., Phoon, K.K., Tang, C., 2022. Hybrid machine learning model with random field and limited CPT data to quantify horizontal scale of fluctuation of soil spatial variability. *Acta Geotech.*
- Zhang, W., Wu, C., Li, Y., Wang, L., Samui, P., 2021a. Assessment of pile drivability using random forest regression and multivariate adaptive regression splines. *Georisk: Assessment and Management of Risk for Engineered Systems and Geohazards* 15, 27–40. <https://doi.org/10.1080/17499518.2019.1674340>
- Zhang, W., Wu, C., Zhong, H., Li, Y., Wang, L., 2021b. Prediction of undrained shear strength using extreme gradient boosting and random forest based on Bayesian optimization. *Geoscience Frontiers* 12, 469–477. <https://doi.org/10.1016/j.gsf.2020.03.007>